

# E ffects of friction on the chiral symmetry restoration in high energy heavy-ion collisions

Masamichi Ishihara and Fujio Takagi<sup>y</sup>

Department of Physics, Tohoku University

Aoba-ku, Sendai 980-8578, Japan

(October 22, 2019)

We study the effects of friction on the chiral symmetry restoration which may take place temporarily in high energy heavy ion collisions. The equations of motion with friction are introduced to describe the time evolution of the chiral condensates within the framework of the linear model. Four types of friction are used to study how the result is sensitive to the choice of the friction. For the thermalization stage, the time dependent temperature is parameterized so as to simulate the result of the parton-cascade model. It is parameterized according to the one dimensional scaling hydrodynamics for the subsequent cooling stage. The time development of the condensates and the entropy production due to friction are calculated numerically. The time interval in which the chiral symmetry is restored approximately is investigated in detail for four types of friction. It is found that; (i) the maximum temperature must be high enough (not lower than 230 MeV) and the friction must be strong enough in order that the chiral symmetry restoration lasts for a long time (not shorter than 3 fm/c); (ii) the ratio of time interval in which chiral symmetry is restored, to the time interval in which the temperature is higher than the critical temperature is typically 0.5 when the friction is strong enough; and (iii) the entropy due to the friction is mainly produced in the early stage of the cooling. The effect of freezeout is discussed briefly.

11.30 Rd, 12.38 M h, 25.75.q

## I. INTRODUCTION

A new phase of matter called quark-gluon-plasma (QGP) is expected to be produced at high energy heavy ion collisions. The chiral symmetry may be restored in the new phase. It is usually claimed that chiral symmetry is restored, i.e. the chiral condensates vanish when the temperature  $T$  of the system is higher than the critical temperature  $T_c$ . However, this is true only when the system is always near the equilibrium. The effective potential may be chirally symmetric if  $T = T_c$ . However, the condition  $T = T_c$  does not necessarily guarantee the vanishing of chiral condensates in a time dependent process because of a finite relaxation time. In our previous work [1] where friction is not taken into account, it was found that the maximum temperature must be high enough for the chiral condensates to vanish temporarily and furthermore the chiral condensates cannot stay near the origin of the chiral space for a long time in general. The reason is as follows. For  $T = T_c$ , the time derivative of the chiral condensates becomes maximum at the bottom of the single-well potential if there is no friction. Then, it is difficult for the condensates to stay near the minimum of the potential for a long time. This implies that the chiral symmetry does not restore for a long time even when  $T$  becomes much higher than  $T_c$ . It may, however, be possible that the condensates stay near the minimum of the potential if there is friction of sufficient magnitude [2, 5]. Therefore, it is important to study the effect of the friction on the motion of the condensates in the chiral space. Here, we consider that the vanishing or very small chiral condensates are the signal of the chiral symmetry restoration.

The chiral symmetry restoration is directly related to the interesting phenomena called disoriented chiral condensates (DCC) [2, 9]. In the conventional scenarios of DCC formation, it is usually assumed that the condensates roll down to the minimum of the temperature dependent effective potential from the top of the hill of the potential. In such scenarios, it is implicitly assumed that the chiral symmetry restoration takes place for a sufficiently long time. Then, it is obvious that the investigation of the chiral symmetry restoration in a dynamical process is important also for studying DCC formation.

In this paper, we investigate whether the chiral condensates can stay near the origin of the chiral space for a long time when the equation of motion has a friction term using the linear model with the massless free particle

---

<sup>x</sup>Electronic address: m.ishihara@nuclphys.tohoku.ac.jp

<sup>y</sup>Electronic address: takagi@nuclphys.tohoku.ac.jp

approximation (MFPA) [8]. The conditions of high energy heavy ion collisions are taken into account through an appropriate initial condition and a time dependent temperature.

This paper is organized as follows. In the next section, we derive the equations of motion for the chiral condensates. Various types of friction are introduced phenomenologically to study its role played in the chiral symmetry restoration in heavy ion collision processes. An expression for the entropy production due to the friction is derived. In section III, the equations of motion are solved numerically for an adequate initial condition and a time dependent temperature. The time interval in which the chiral symmetry is restored approximately is studied in detail. Entropy production is also studied. Section IV is devoted to conclusions and discussions.

## II. THE LINEAR MODEL AND THE EQUATION OF MOTION WITH FRICTION

### A. Equation of motion

The linear model is a useful tool to investigate the time evolution of the chiral condensates. The Lagrangian is

$$L = \frac{1}{2} \partial_i \partial_j - \frac{1}{4} v^2 + H; \quad (1)$$

where  $\partial_i = (\partial; \sim)$  and  $v^2 = (v_0; v_1; v_2; v_3) = \sum_{j=0}^3 v_j^2$ . The equation of motion for the field  $v_i$  is

$$2 \partial_i \partial_j v^2 - v_i H_{ij0} = 0; \quad (2)$$

The field  $v_i$  is divided into two parts, the condensate  $v_i = h_i v_i$  which is the expectation value of the field  $v_i$  and the fluctuation  $\tilde{v}_i = v_i - h_i$ . Then, we obtain

$$2 \partial_i \partial_j v^2 - v_i H_{ij0} + 2 \tilde{v}_i + m_i^2 \tilde{v}_i + 4 \tilde{v}_i^2 + 2 \sum_{j \neq i}^3 \tilde{v}_j \tilde{v}_j^5 = 0; \quad (3)$$

where  $m_i^2 = 2 \tilde{v}_i^2 + v_i^2$ .

In eq.(3), we take the normal ordering with respect to the vacuum for which the expectation value of  $v_i$  is  $h_i$ . Assuming that the fluctuation fields  $\tilde{v}_i$  are in the thermal equilibrium, we obtain the following equation of motion:

$$2 \partial_i \partial_j v^2 - v_i H_{ij0} + h_i \tilde{v}_i^2 + 2h_i \tilde{v}_i^2 = 0; \quad (4)$$

Note that the thermal average of the third order term in  $\tilde{v}_i$  is vanishing under the free particle approximation. On the other hand, the thermal average of the  $\tilde{v}_i^2$  is given by

$$h_i \tilde{v}_i^2 = \frac{1}{(2\pi)^3 k_i!} \frac{1}{\exp(-\epsilon_i/T)}; \quad (5)$$

where  $\epsilon_i = \sqrt{k_i^2 + m_i^2}$ . It is equal to  $T^2 = 12$  for  $m_i = 0$ . As a result, the equation of motion of condensates under MFPA [8] turns out to be

$$2 \partial_i \partial_j v^2 + \frac{T^2}{2} v_i H_{ij0} = 0; \quad (6)$$

One can see from eq.(6) that the potential for the condensates is given by

$$V(v; v_0; T) = \frac{1}{4} v^2 + \frac{T^2}{2} H_{00}; \quad (7)$$

We define the temperature dependent mass squared by the second derivative of  $V(v; v_0; T)$ :

$$M_i(v; v_i; T)^2 = \frac{d^2 V}{d v_i^2} = v^2 + \frac{T^2}{2} + 2 \tilde{v}_i^2; \quad (8)$$

As already mentioned in Sec.I, the aim of this paper is to investigate the friction effects on the chiral symmetry restoration in high energy heavy ion collisions. The system which consists of the chiral condensates (soft modes) will be far from a (local) thermal equilibrium in such a time dependent process even when the environment which consists of the fluctuation fields (hard modes) is approximately in the (local) thermal equilibrium. In such a case, a friction term appears in general as a result of the dissipation-fluctuation theorem [11]. Thus we use a phenomenological equation of motion with a friction term :

$$2 \dot{v}_i + \frac{T^2}{2} v_i^2 - H_{i,0} + \sum_j \frac{X_{ij}}{m_j} \frac{dv_j}{dt} = 0; \quad (9)$$

Here,  $X_{ij}$ 's are the friction coefficients. In general, the friction coefficients depend on both  $T$  and  $v_i$ . In this paper, we assume that  $X_{ij} = \gamma_{ij}$ . For the functional form of  $\gamma$  which may provide either  $T$  and/or  $v_i$  dependence, we use the following form which was obtained for the chirally symmetric vacuum [2,3] (See also, [12]):

$$\gamma = \frac{9}{16} \frac{2T^2}{m} f_{Sp} \left( 1 - e^{\frac{m}{T}} \right) F(m;T); \quad (10)$$

where  $f_{Sp}(x) = \frac{R_x}{1} \frac{dt}{t} \frac{\ln t}{t^2}$  is the Spence function and  $m$  is the temperature dependent mass. In this paper, we consider the following four cases as the choice of  $\gamma$  :

case A :

$$\gamma = \text{constant}; \quad (11a)$$

i.e.  $\gamma$  is taken for simplicity as a constant which is independent of both  $T$  and  $v_i$  [2,5]

case B :

$$\gamma = F(m;T); \quad (11b)$$

where  $m$  is the pion mass at zero temperature. This choice may serve as a case in which  $\gamma$  has the simplest nontrivial  $T$ -dependence. This case may be realized in the rapid cooling case.

case C :

$$\gamma = F(M_3(f;0;T);T); \quad (11c)$$

This is another case where  $\gamma$  has a simple  $T$ -dependence. In this case, we ignore the change of  $m$  in the  $v$ - and  $T$ -dependent mass defined in eq.(8), i.e., we take  $\gamma_0 = f$  and  $\gamma_i = 0$  for  $i = 1, 2, 3$  in order that  $M_3(f;0;T)$  coincides with the pion mass at  $T = 0$ .

case D :

$$\gamma = F(M_3(v;0;T);T); \quad (11d)$$

where  $v$  is the condensation value of the temperature dependent vacuum which is determined by the extremum condition

$$\frac{\partial V}{\partial v} = \frac{\partial V}{\partial v} \Big|_{v=0} = 0; \quad (11e)$$

In this case, the mass  $M_3$  depends on both  $T$  and  $v$  while the latter is a function of  $T$ . Note that only case A has been considered by previous authors in numerical analyses [2].

The magnitude of the friction may be estimated from eq.(10) for the symmetric phase. Biro and Greiner suggested that  $\gamma = 2.2 \text{ fm}^{-1}$  at  $T = T_c$  [2]. Rischke calculated  $\gamma$  for the broken phase [3]. It was also estimated by Yabu et al. [4] using the Caldeira-Legegett method. Their result is  $\gamma = 0.7 \text{ fm}^{-1}$  in the uniform case. For the case A, we use  $\gamma = 2 \text{ fm}^{-1}$  as a typical value and consider also some other values for comparison. Considering the theoretical ambiguity in the magnitude of  $\gamma$ , we introduce the overall multiplicative constant  $C$  for cases B, C and D. The friction coefficient  $\gamma$  in these three cases are replaced with  $C \gamma$  with various  $C$  in the following numerical calculations.

### C . Temperature dependence of temperature

We consider the time development of chiral condensates in the entire stage of heavy ion collisions at high energies. We concentrate on the central rapidity region where the temperature will be highest. A process which takes place in this region will be approximately invariant under the Lorentz boost along the collision axis. Then a convenient variable is the proper time  $\tau$ . The condensates which are formed in the central region will evolve under the influence of the environment which consists of any number of partons (quarks, antiquarks and gluons) or hadrons. The effect may be represented by the temperature  $T$  which depends on the proper time  $\tau$  provided the environment is in the local thermal equilibrium [1]. We use the temperature as a convenient parameter even for the very early stage of the collision process where the environment may be far from the thermal equilibrium. This is because we do not know any other reliable method to describe the effect of the environment in the pre-equilibrium stage.

It is conceivable that hard collisions among the incident partons play a crucial role to thermalize the system in the beginning of the entire process. We then borrow the result of the parton cascade model [13] in order to parameterize the dependence of  $T$  for the early thermalization stage including the very early stage of the collision. It is possible to estimate the  $\tau$ -dependent temperature  $T(\tau)$  up to  $\tau = \tau_m$  when the temperature reaches the maximum  $T_m$  using the energy densities calculated in [13] with the equation of state for the free quark-gluon gas. For example, one has  $T_m = 620$  MeV and  $880$  MeV for Au-Au collisions at RHIC and LHC energies, respectively. The proper time  $\tau_m$  is typically some 1 fm. After this time, the system will expand mainly along the collision axis. The one-dimensional scaling hydrodynamics [14] will be a good approximation for the cooling stage. Then the temperature becomes a function of  $x$  only,  $T = T(x)$  for  $x > \tau_m$ . To summarize, the temperature is parameterized as follows as a function of the scaled proper time  $x = \tau/\tau_m$  for the entire stage of the collision [1]:

$$T(x) = T_i \left( \frac{T_m}{T_i} \right)^{\frac{x}{\tau_m}} (1 - x) + T_m x^{1/3} (x - 1); \quad (12)$$

The temperature parameterized in eq.(12) stays finite for a long time. However, the interactions between the environment and the condensates will vanish at a certain temperature called the freezeout temperature  $T_f$ . Therefore, it is reasonable to consider that  $T$  suddenly becomes zero when it reaches  $T_f$ . Then, the time dependence of the temperature may be parameterized as

$$T(x) = T_i \left( \frac{T_m}{T_i} \right)^{\frac{x}{\tau_m}} (1 - x) + T_m x^{1/3} (x - 1) (x_f - x); \quad (13)$$

where  $x_f = (T_m/T_f)^3$  and  $\tau_f = x_f \tau_m$  being the freezeout time. To summarize, the temperature decreases from  $T_m$  down to  $T_f$  and then suddenly becomes zero. It is supposed that the friction vanishes after  $x_f$  because there will be no energy dissipation from the condensates into the thermal environment after the freezeout. In this situation, the initial condition of the quench scenario for the formation of DCC [6,7] may be realized at  $x = x_f$ . On the other hand, a whole process may exhibit a characteristic feature of the annealing scenario [7,8] if  $T_f$  is much lower than  $T_c$  and if the one-dimensional expansion lasts for a long time. Equation of motion, eq.(9), is now rewritten as

$$\frac{\partial^2}{\partial t^2} + \frac{1}{\tau} \frac{\partial}{\partial t} + \frac{1}{2} v^2 + \frac{T^2(x)}{2} - v^2 \frac{\partial}{\partial t} H_{i,0} + \frac{\partial}{\partial t} H_{i,0} = 0; \quad (14)$$

where we assume that the system is homogeneous along the transverse direction. In the next section, eq.(14) will be solved numerically with  $T(x)$  given by eq.(12) or eq.(13).

### D . Entropy production

Consider the following equation of motion of a particle with mass  $m$  in order to find the expression for the entropy production:

$$m \frac{d^2 X}{dt^2} = F(X) + G(X); \quad (15)$$

where  $F(X)$  represents a conservative force and  $G(X)$  a non-conservative one. The work  $W$  which the particle does by  $G(X)$  is

$$W = \int_c^Z dX G(X); \quad (16)$$

where  $c$  is the path of the particle. If the work  $W$  is fully converted into heat, the produced entropy is given by

$$S = \int_c^Z \frac{dQ}{T} = \int_c^Z dX \frac{G(X)}{T} = \int_c^Z dt \frac{dX}{dt} \frac{G(X)}{T}; \quad (17)$$

In the present case,  $X$  corresponds to  $\frac{d}{dt} \ln \frac{d_i}{d_j}$  and  $G(X)$  to  $\frac{P}{T} \ln \frac{d_i}{d_j}$ . Then, The increase in the entropy density may be given by

$$ds_i = \frac{X}{j} d_i \frac{d_j}{d_i} = d \frac{X}{j} \frac{d_j}{d_i} = d \frac{d_i}{d} \frac{d_j}{d}; \quad (18)$$

where  $t$  has been replaced with  $\ln \frac{d_i}{d_j}$ . The above expression is in agreement with eq.(4.6) in ref. [10] when there is only one kind of field. The entropy density production per unit proper time is given by

$$\frac{ds_i}{d} = \frac{X}{j} \frac{d_j}{d_i} \frac{d_i}{d} = \frac{d_j}{d}; \quad (19)$$

### III. NUMERICAL RESULTS

#### A. Choice of parameters

We take the parameters of the linear model as follows in the following numerical calculations:  $\mu = 20$ ,  $v = 87.4$  and  $H^{1/3} = 119$  MeV. This set of the parameters generates the pion mass 135 MeV, the sigma mass 600 MeV and the pion decay constant  $f = 92.5$  MeV. The initial condition of the equation of motion, eq.(14), is taken as

$$0; \tilde{v} = f; \tilde{v}; \quad (20a)$$

$$\frac{d_0}{d}; \frac{d_1}{d}; \frac{d_2}{d}; \frac{d_3}{d} = \frac{T_i^2}{30}; \frac{T_i^2}{30}; \frac{T_i^2}{30}; \frac{T_i^2}{30}; \quad (20b)$$

where  $T_i$  is the initial temperature.

Four types of friction given in eqs. (11a) – (11d) are used in the following calculations. The  $T$ -dependence of the friction in cases B, C and D is displayed in Figs.1a and 1b. The  $T$ -dependence in the case D comes from the  $T$ -dependence of the pion mass. The pion mass is almost constant below  $T_c$  and increases linearly above  $T_c$ . This behavior of the pion mass below  $T_c$  is similar to that in case B. The behavior above  $T_c$  is asymptotically identical to that in case C. Moreover, the magnitude of the friction is determined mainly by the factor  $T^2/m(T)$ . As a result, the  $T$ -dependence of the friction in case D is quite similar to that in case B at low temperatures and it is similar to that in case C at high temperatures. The  $T$ -dependence of the friction in case D has a peak near the  $T_c$  because of  $T$ -dependence of the pion mass. Since the  $T$ -dependence of the friction comes from the  $T$ -dependence of the pion mass, that in case B is proportional to  $T^2$ , while that in case C and D is proportional to  $T$  at high temperatures.

#### B. Time development of chiral condensates

We have solved eq.(14) numerically for various types of friction. The result for case A with the maximum temperature  $T_m = 200$  MeV, the initial temperature  $T_i = 1$  MeV, the time  $t_m = 1$  fm and various  $\mu$  is shown in Fig.2. It is found that a) the motion of the condensates for  $x < 1$  is insensitive to the value of  $\mu$ , and b) the condensates cannot stay for a sufficiently long time in the center of the chiral space. As already found in [1], a characteristic damped oscillation appears in the no friction case ( $\mu = 0$ ). Contrary to this, the oscillation diminishes rapidly when  $\mu = 1$  and  $2 \text{ fm}^{-1}$ . The condensates ( $\phi_0$ ) in these two cases pass near the center of the oscillation in the  $\mu = 0$  case.

The time development of condensates in cases B, C and D with  $T_m = 250$  MeV,  $T_i = 1$  MeV and  $t_m = 1$  fm is shown in Fig.3. There are characteristic oscillations in cases C and D, while there is not in case B. The oscillation in case D

is weaker than that in case C. These different behaviors reflect the different  $T$ -dependence of the friction in the three cases.

The  $T_m$  dependence of the condensate  $\phi$  in case A is shown in Fig.4, where the parameters are taken as  $T_i = 1$  MeV,  $m = 1$  fm and  $\gamma = 2\text{fm}^{-1}$ . Higher the maximum temperature is, faster it moves to the origin. However, it is difficult to be stopped by friction as the condensate moves rapidly. The different behavior for  $x = 10$  is due to the difference of  $T$ . Since the behavior of  $T$  is determined by the scaling property,  $T$  depends on only  $T_m$  if  $m$  is fixed. Higher  $T$  is, smaller the minimum of the potential (eq.(7)) is. As a result, the condensate is small for high  $T_m$ .

The sensitivity of the time development to the initial temperatures  $T_i$  is shown in Fig.5. It is found that the  $T_i$  dependence is weak.

The proper time  $\tau_m$  is 1 fm or less according to the result of the parton cascade model. The condensates evolves in a different way for different  $m$  even if other parameters,  $T_m$ ;  $T_i$  and  $\gamma$  are fixed. Since  $m$  determines the behavior of the temperature in the entire stage, we show typical  $m$  dependence in Fig.6 for  $T_m = 250$  MeV,  $T_i = 1$  MeV and  $\gamma = 2\text{fm}^{-1}$ . For  $x < 10$ , the time development in  $x$  is faster for larger  $m$ . On the other hand, the behavior for  $x > 14$  is almost independent of  $m$ . That is, the behavior at large  $x$  scales in  $x$ . The motion at large  $x$  is determined solely by  $T$  for given  $T_m$ ;  $T_i$  and  $\gamma$ .

The effect of freezeout on the time development of condensates in case D is demonstrated in Fig.7. The curves (—) and (—) represent the results obtained with the time dependent temperature (12) and (13), respectively. Of course, the effect of freezeout is seen only for  $x > x_f$ . For comparison,  $T(x)$  given by eq.(13) is also shown in Fig.7. The center of the oscillation of sigma condensate in the curve (—) is almost fixed. The amplitude of the oscillation is determined by the magnitude of the condensate at the freezeout time.

### C. Chiral symmetry restoration time

One may claim that the chiral symmetry is restored approximately if every  $j_{\perp}$  becomes much smaller than  $v$ . For definiteness, we use the following condition to define the approximate restoration of chiral symmetry:

$$p_{\perp}^2 = v^2 \quad 0.2: \quad (21)$$

From now on, we say that chiral symmetry is restored if the condition (21) is satisfied.

We take  $T_i = 1$  MeV and  $m = 1$  fm in the following calculations. Time interval  $\tau$  in which chiral symmetry is approximately restored is calculated for the four cases with various  $T_m$ . The result for case A is shown in Fig.8. It is found that the condition  $T_m > 230$  MeV,  $\gamma > 1\text{fm}^{-1}$  must be fulfilled in order that  $\tau > 3$  fm. At fixed  $\gamma$ , higher  $T_m$  is, longer  $\tau$  becomes. This is because the condensates moves to the minimum of the potential (namely to the chiral vacuum) rapidly and high temperature era when  $T > T_c$  lasts for a long time when  $T_m$  is high. On the other hand, for fixed  $T_m$ ,  $\tau$  increases as a function of  $\gamma$  for small  $\gamma$ , reaches a maximum at some  $\gamma$  and then decreases. This behavior is understood as follows. If  $\gamma$  is large, the condensate moves slowly and almost stops near the origin resulting in a long  $\tau$ . However, if  $\gamma$  is too large,  $T$  becomes lower than  $T_c$  before the condensate reaches the origin and hence,  $\tau$  becomes short. The same tendency is found in other cases.

The result for the case B is shown in Fig.9. Now  $\tau$  is plotted as a function of  $C$  introduced in subsection II B. The condition for having  $\tau > 3\text{fm}^{-1}$  is  $T_m = 250$  MeV and  $C > 0.1$ . In this case, large  $\tau$  can be realized even when  $C$  is very small because  $T$  becomes very large. (See Fig.1b) The result for case C is shown in Fig.10. The appearance of large  $\tau$  for  $T_m = 140$  MeV is due to an accidental fluctuation. Maximum temperature must be higher than 260 MeV and  $C$  must be larger than 2 in order that  $\tau > 3$  fm. Fig.11 shows the time interval in case D. The condition for having  $\tau > 3$  fm is  $T_m = 220$  MeV and  $C > 1.5$ —2.0. To summarize the results for the four cases, we found the following general tendency common to every case: (a) the  $T_m$  dependence of  $\tau$  is approximately universal as long as the friction is sufficiently but not too strong; (b)  $T_m$  must be larger than 220—260 MeV in order to have  $\tau > 3$  fm; (c) approximate chiral symmetry restoration does not take place if the friction is very small.

We define the time interval  $\tau_c$  in which the temperature of the system is higher than the critical temperature  $T_c$  in order to compare it with  $\tau$ . It is given by

$$\tau_c = m \left( \frac{T_m}{T_c} \right)^{3/2} \quad 1: \quad (22)$$

This ratio in case A is shown in Fig.12. It is found that the typical value of this ratio is about 0.5. Each of the lines corresponds to various  $T_m$  ranging from 230 MeV to 390 MeV. The ratio is approximately independent of  $\gamma$  for large  $\gamma$ . We have confirmed that these features are common to all the four cases.

Finally, the entropy production due to the friction is calculated. The result for case D is already shown in g.7. For comparison, we have calculated it for case A with  $\gamma = 2 \text{ fm}^{-1}$ ,  $T_m = 250 \text{ MeV}$ ,  $T_i = 1 \text{ MeV}$  and  $m = 1 \text{ fm}$ . The result is shown in Fig.13. It is found that entropy is produced mainly in the early cooling stage. Entropy production lasts for a relatively short time (a few fm) and hence it is not affected by the freezeout. The entropy production is mainly due to the motion of  $\pi_0$  condensate

#### IV . CONCLUSIONS AND DISCUSSIONS

The time development of chiral condensates in high energy heavy ion collisions are calculated with the adequate initial conditions and frictions. The linear model with four types of friction are used. The main results are: a) the characteristic damped oscillation of the condensates in no friction case is smeared by the friction; b) sufficiently high maximum temperature ( $T_m = 220 \text{ MeV}$ ) and the friction of appropriate magnitude are needed for the vacuum to be chiral symmetric for a sufficiently long time ( $\tau = 3 \text{ fm}$ ); c) entropy is produced mainly in the early stage of the cooling.

For each friction type, we found the following results. In case A, the constant friction which has been used by some authors generates the largest  $\tau$  among four cases. However, it is not clear whether the  $T$  independence of  $\tau$  is a good approximation or not. In case B,  $\tau$  is long enough even for small  $C$ . However, the magnitude of the friction is unrealistically large at high temperatures. In case C,  $\tau$  is small for the realistic range of the friction ( $0.5 \leq C \leq 3$ ). In case D, large  $\tau$  is obtained for the possible range of the friction ( $0.5 \leq C \leq 3$ ). The peak of  $\tau$  near  $T_c$  (see Fig.1a) is responsible for large  $\tau$  in this case.

As stated in the introduction, the conventional scenarios of the formation of QGP and DCC in which the chiral symmetry is supposed to be restored for a sufficiently long time are not always guaranteed. Our results suggests that it is important to estimate precisely the maximum temperature of the system and the friction for the soft mode.

In general scenarios of QGP evolution, it is well-known that the entropy of the system is mostly produced in the thermalization stage ( $x = 1$ ). However, we found that the entropy due to the friction felt by the condensates is produced in the early stage of the cooling.

As the initial condition of conventional DCC formation scenarios, it is often assumed that the roll-down of chiral condensates starts from the top of the potential (chirally symmetric vacuum) and the initial temperature is close to  $T_c$ . However, this initial condition may not be always satisfied as the chiral symmetry restoration does not necessarily occur even when the temperature of the system exceeds  $T_c$ .

In our calculation, the condensation dependence of the friction is included in case D. However, it reflects essentially only the  $T$ -dependence of the vacuum. The effect of the time dependent condensates is not taken into account yet. Such a dependence [3] should be included to refine the analysis. On the other hand, random forces are not considered also in the present paper. They generate fluctuations in the motion of the condensates and hence in  $\tau$ . The massless free particle approximation is not reliable at low temperature. The effects of mass and the finite volume of the colliding system have to be taken into account to improve the theory. However, we believe that our results are correct at least qualitatively. The problems listed above and their effects on DCC formation will be discussed in the coming paper.

- [1] M . Ishihara and F . Takagi, Phys. Rev. C 59, 2221 (1999) .
- [2] T S. Biro and C . G reiner, Phys. Rev. Lett. 79, 3138 (1997) .
- [3] D H . R ischke, Phys. Rev. C 58, 2331 (1998) .
- [4] H . Yabu, K . N ozawa and T . Suzuki, Phys. Rev. D 57, 1687 (1998) .
- [5] S. D igal, R . R ay, S. Sengupta and A M . Srivastava, hep-ph/9805227 ; A K . Chaudhuri, Phys. Rev. D 59, 117503 (1999) ; A K . Chaudhuri, hep-ph/9904269 .
- [6] K . Rajagopal and F . W ilczek, Nucl. Phys. B 404, 577 (1993) ; S. G avin, A . G ocksch and R D . Pisarski, Phys. Lett. 72, 2143 (1994) ; J-P . B laizot and A . K rzywicki, Phys. Rev. D 50, 442 (1994) ; A . B ialas, W . C zyz, and M . G myrek, ibid. 51, 3739 (1995) ; D . B oyanovsky, H . J. de Vega and R . Holman, ibid. 51, 734 (1995) ; A . Abada and M . C . B irse, ibid. 57, 292 (1998) ; D . M olnar, L P . C semai and Z . I . Lazar, ibid. 58, 114018 (1998) .
- [7] M . A sakawa, Z . H uang and X . N . W ang, Phys. Rev. Lett. 74, 3126 (1995) .
- [8] S. G avin and B . M uller, Phys. Lett. B 329, 486 (1994) .

[9] A.A. Anselm and M.G. Ryskin, Phys. Lett. B 266, 482 (1992) ; Z. Huang, M. Suzuki and X.N. Wang, Phys. Rev. D 50, 2277 (1994) ; T.D. Cohen, M.K. Banerjee, M.N. Nielsen and X. Jin, Phys. Lett. B 333, 166 (1994) ; R.D. Amado and I.I. Kogan, Phys. Rev. D 51, 190 (1995) ; F. Cooper, Y.K. Lüger, E.M. Ottola and J.P. Paz, *ibid.* 51, 2377 (1995) ; M.A. Lamport, J.F. Dawson and F. Cooper, *ibid.* 54, 2213 (1996) ; J. Randrup, Phys. Rev. Lett. 77, 1226 (1996) ; J.I. Kapusta and A.P.V. Ischer, Z. Phys. C 75, 507 (1997) ; G. Amelino-Camelia, J.D. Björken and S.E. Larsson, Phys. Rev. D 56, 6942 (1997) ; M. Ishihara, M. Maruyama and F. Takagi, Phys. Rev. C 57, 1440 (1998) ; H. Hirooka, H. Minakata, Phys. Lett. B 425, 129 (1998) ; Erratum *ibid.* B 434, 461 (1998) ; B.K. Nandi, T.K. Nayak, B.M. Chanty, D.P. Mahapatra, Y.P.V. Iyogi, nucl-ex/9903005 .

[10] A. Hosoya and M. Sakagami, Phys. Rev. D 29, 2228 (1984) .

[11] M. Morikawa, Prog. Theor. Phys. 93, 685 (1995) ; C.G. Reinier and B.M. Uller, Phys. Rev. D 55, 1026 (1997) ; A.N. Iegawa, hep-th/9810043 ; E.A. Calzetta and B.L. Hu, Phys. Rev. D 59, 065018 (1999) .

[12] S. Joen, Phys. Rev. D 52, 3591 (1995) .

[13] K. G. Eiger, Phys. Rev. D 46, 4986 (1992) .

[14] J.D. Björken, Phys. Rev. D 27, 140 (1983) .

FIG. 1a. The temperature dependence of the magnitude of friction in cases B, C and D .

FIG. 1b. The temperature dependence of the magnitude of friction in cases B, C and D . Note that the scale of  $T$  is different from that in Fig. 1a.

FIG. 2. The development of chiral condensates for various magnitudes of friction with  $T_m = 200$  MeV,  $T_i = 1$  MeV and  $m = 1$  fm in case A

FIG. 3. The development of chiral condensates for  $T_m = 250$  MeV,  $T_i = 1$  MeV and  $m = 1$  fm in cases B, C and D .

FIG. 4. The development of chiral condensates for various  $T_m$  with  $T_i = 1$  MeV,  $m = 1$  fm and  $= 2$  fm<sup>1</sup> in case A .

FIG. 5. The development of chiral condensates for various  $T_i$  with  $T_m = 250$  MeV,  $m = 1$  fm and  $= 2$  fm<sup>1</sup> in case A .

FIG. 6. The development of chiral condensates for various  $m$  with  $T_m = 250$  MeV,  $T_i = 1$  MeV and  $= 2$  fm<sup>1</sup> in case A .

FIG. 7. The development of sigma condensate and entropy production per unit scaled time ( $= m$ ) without ( ) and with ( ) the freezeout in case D . The parameters are  $T_m = 250$  MeV,  $T_i = 1$  MeV,  $m = 1$  fm and  $T_f = 90$  MeV .

FIG. 8. The time interval ( $\tau$ ) in which chiral symmetry restoration lasts longer than 3 fm for various  $T_m$  with  $T_i = 1$  MeV and  $m = 1$  fm in case A .

FIG. 9. The time interval ( $\tau$ ) in which chiral symmetry restoration lasts longer than 3 fm for various  $T_m$  with  $T_i = 1$  MeV and  $m = 1$  fm in case B . It is displayed for (a) 0 C 1 and (b) 0 C 3.

FIG. 10. The time interval ( $\tau$ ) in which chiral symmetry restoration lasts longer than 3 fm for various  $T_m$  with  $T_i = 1$  MeV and  $m = 1$  fm in case C . It is displayed for (a) 0.5 C 3 and (b) 0 C 20.

FIG. 11. The time interval ( $\tau$ ) in which chiral symmetry restoration lasts longer than 3 fm for various  $T_m$  with  $T_i = 1$  MeV and  $m = 1$  fm in case D . It is displayed for (a) 0 C 3 and (b) 0 C 20.

FIG. 12. The ratio  $r = c$  for various  $T_m$  in case A.

FIG. 13. Entropy production per unit scaled time ( $= m$ ) without the freezeout with  $T_m = 250$  MeV,  $T_i = 1$  MeV,  $m = 1$  fm and  $\gamma = 2$  fm $^{-1}$  in case A.

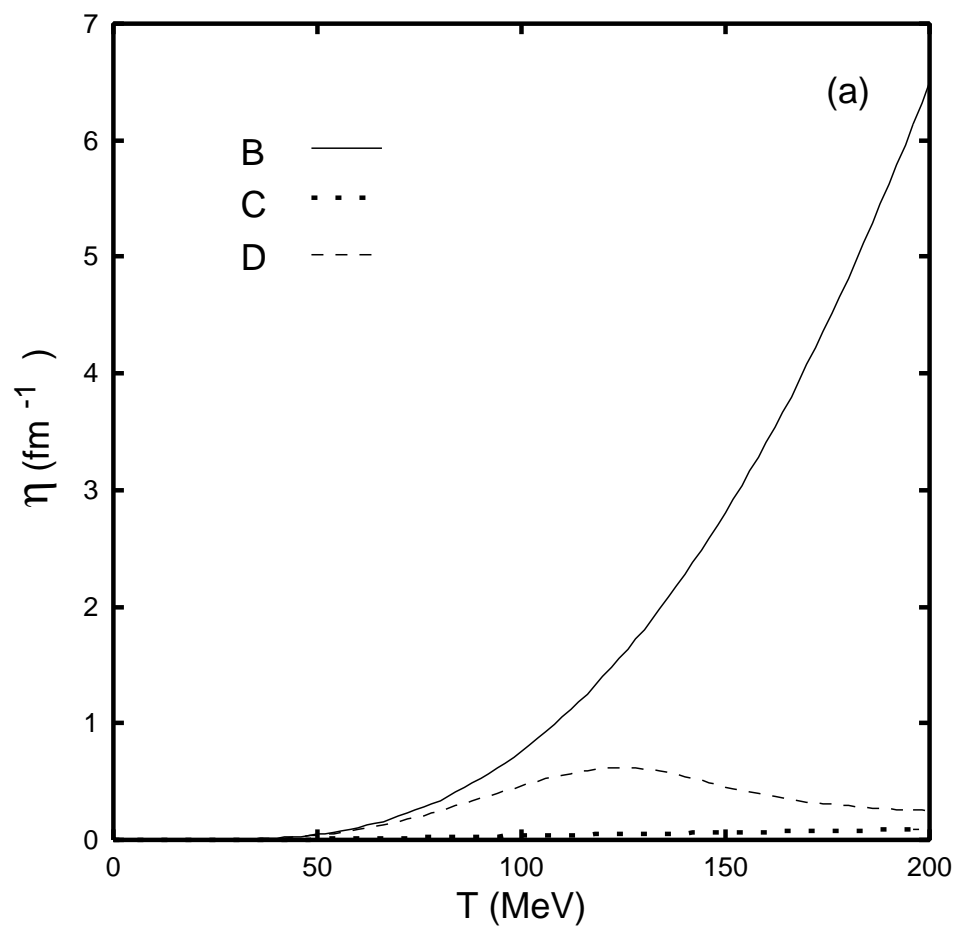


Fig.1a



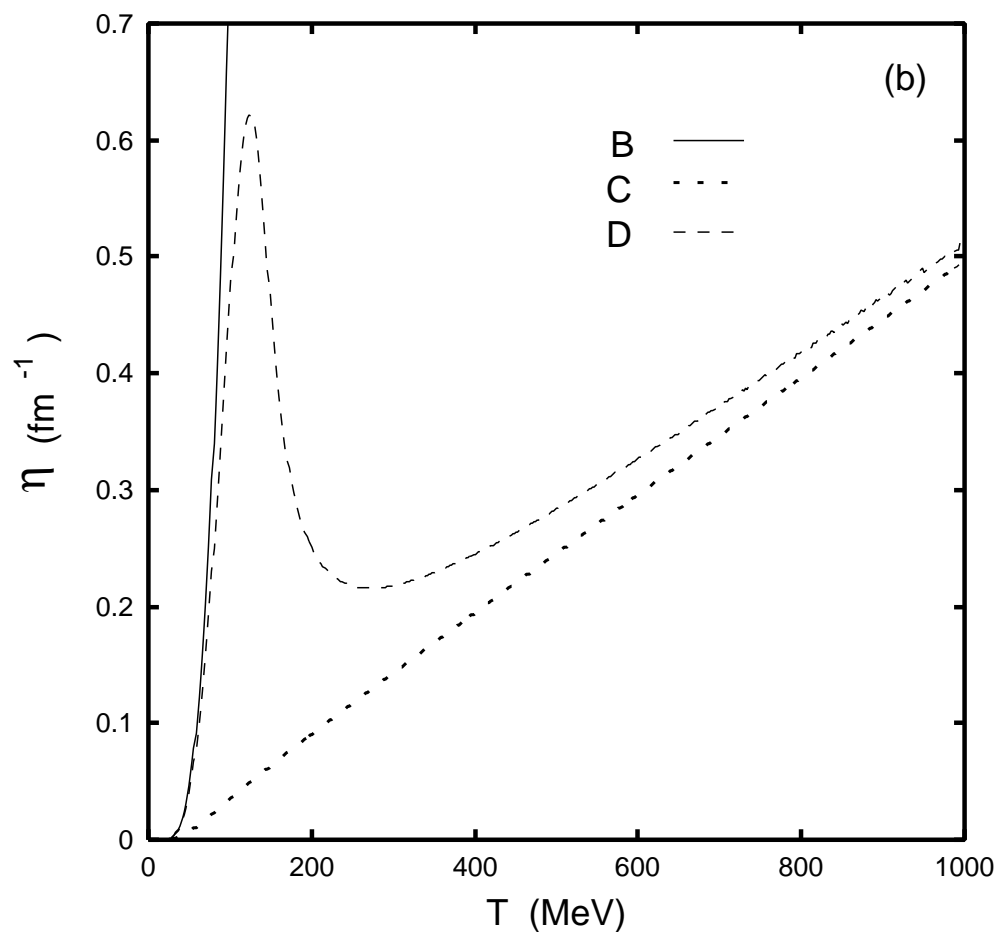


Fig.1b



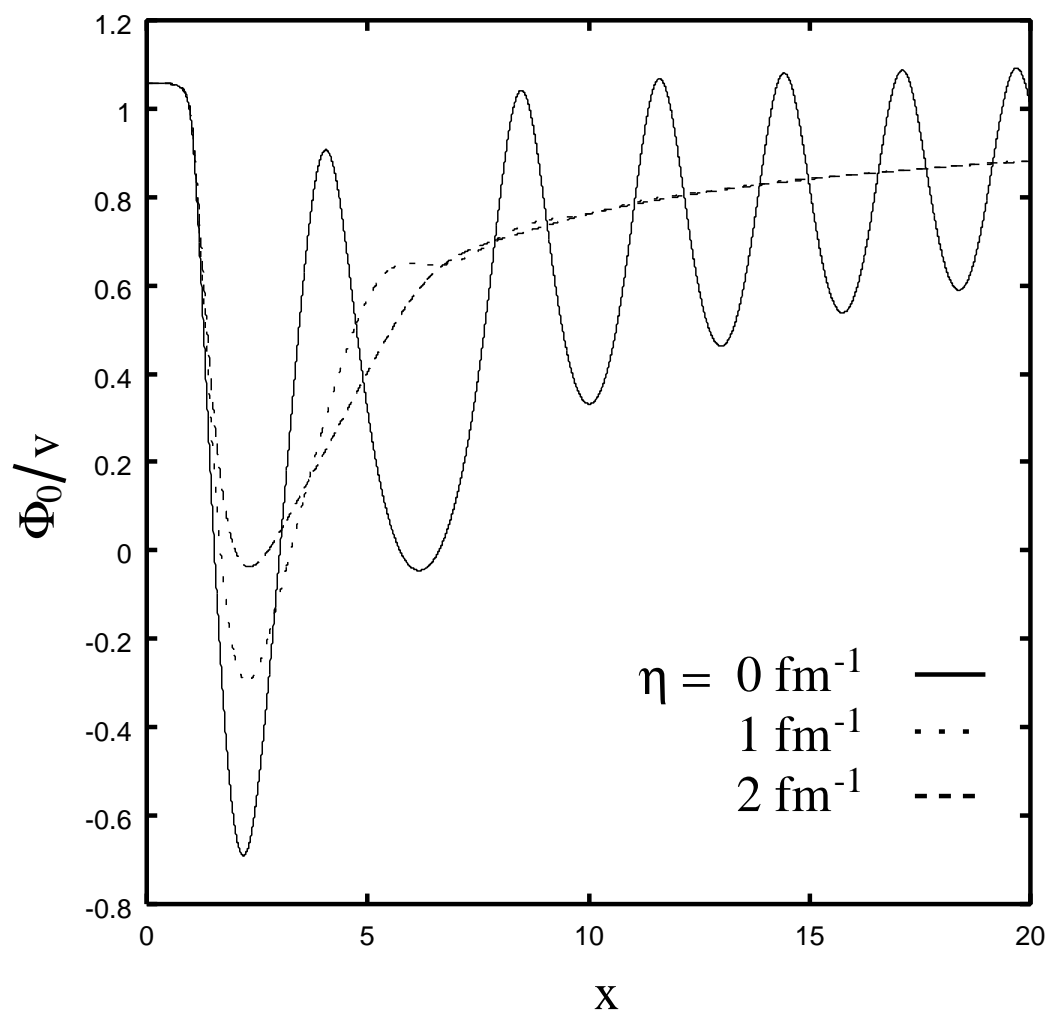


Fig.2



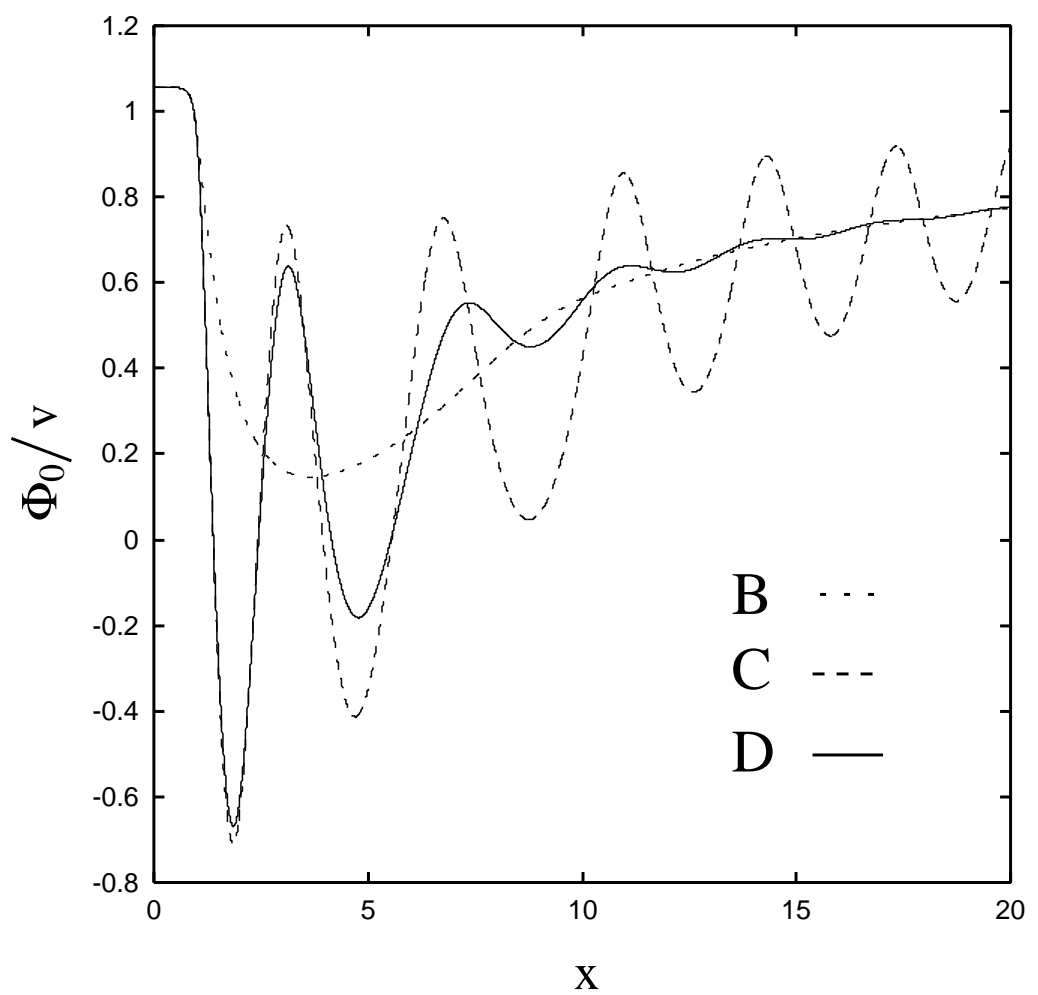


Fig.3



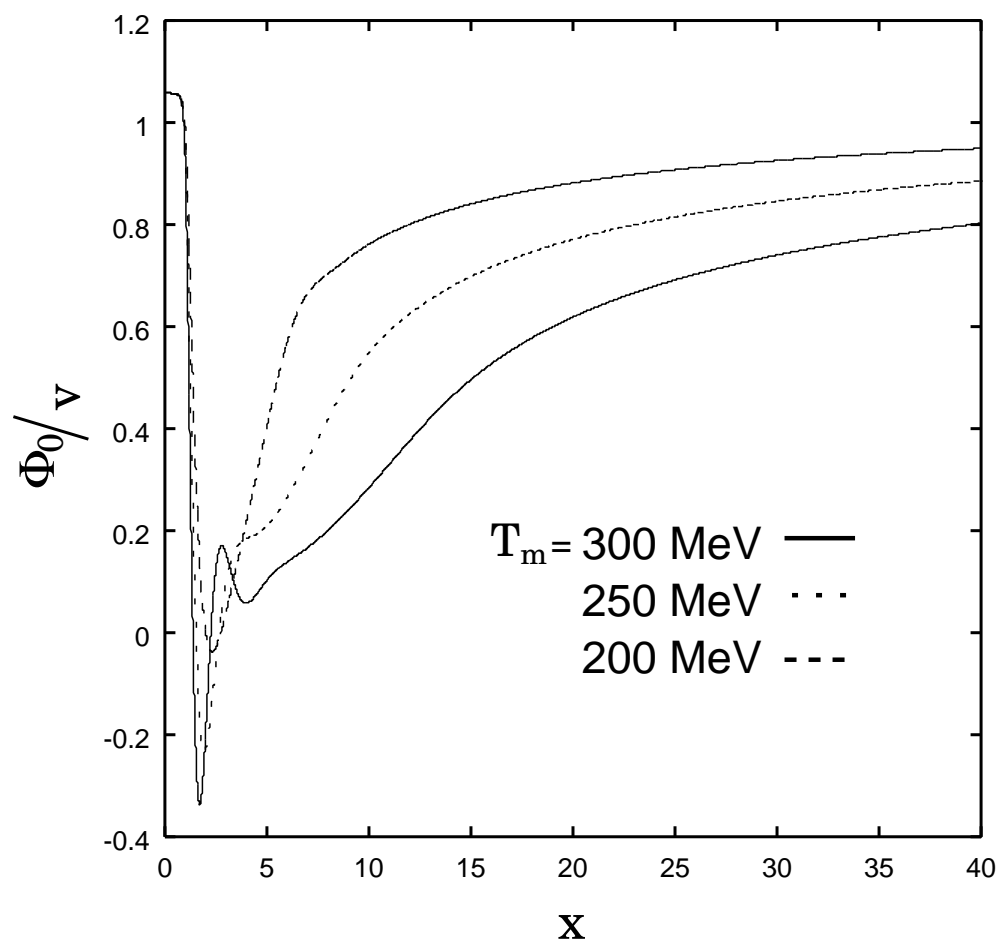


Fig.4



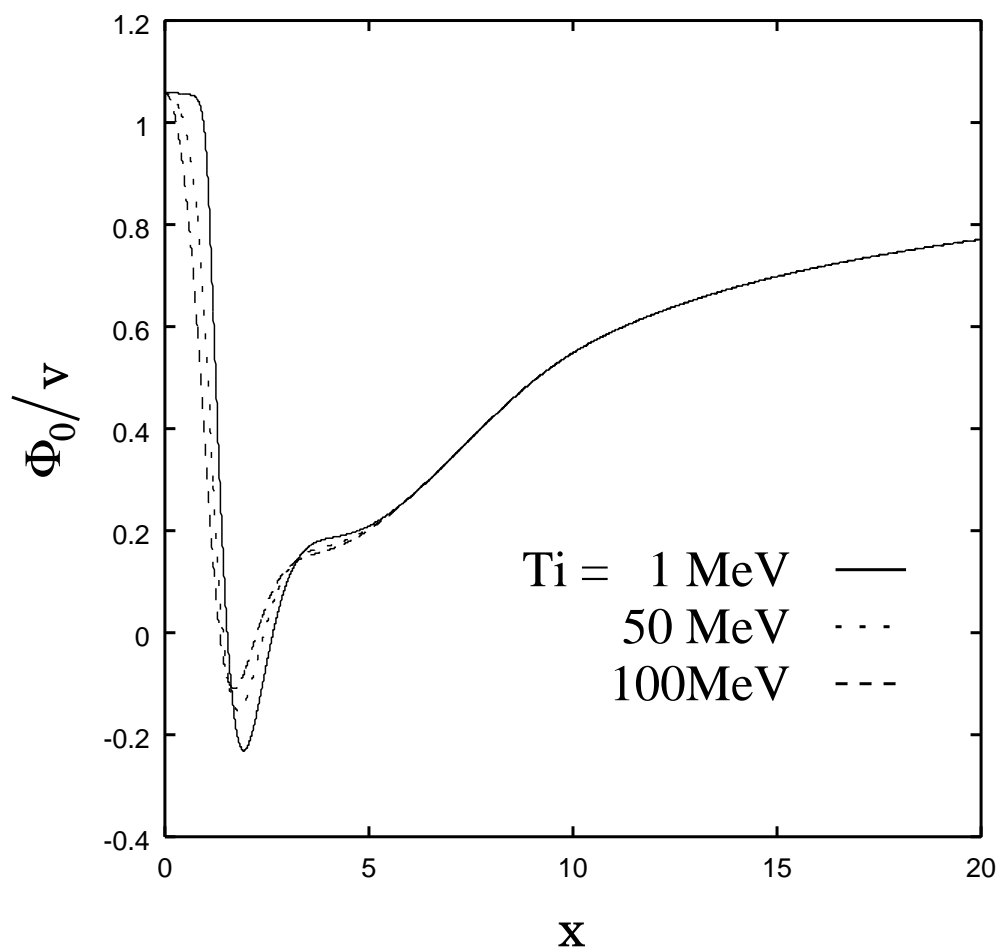


Fig.5



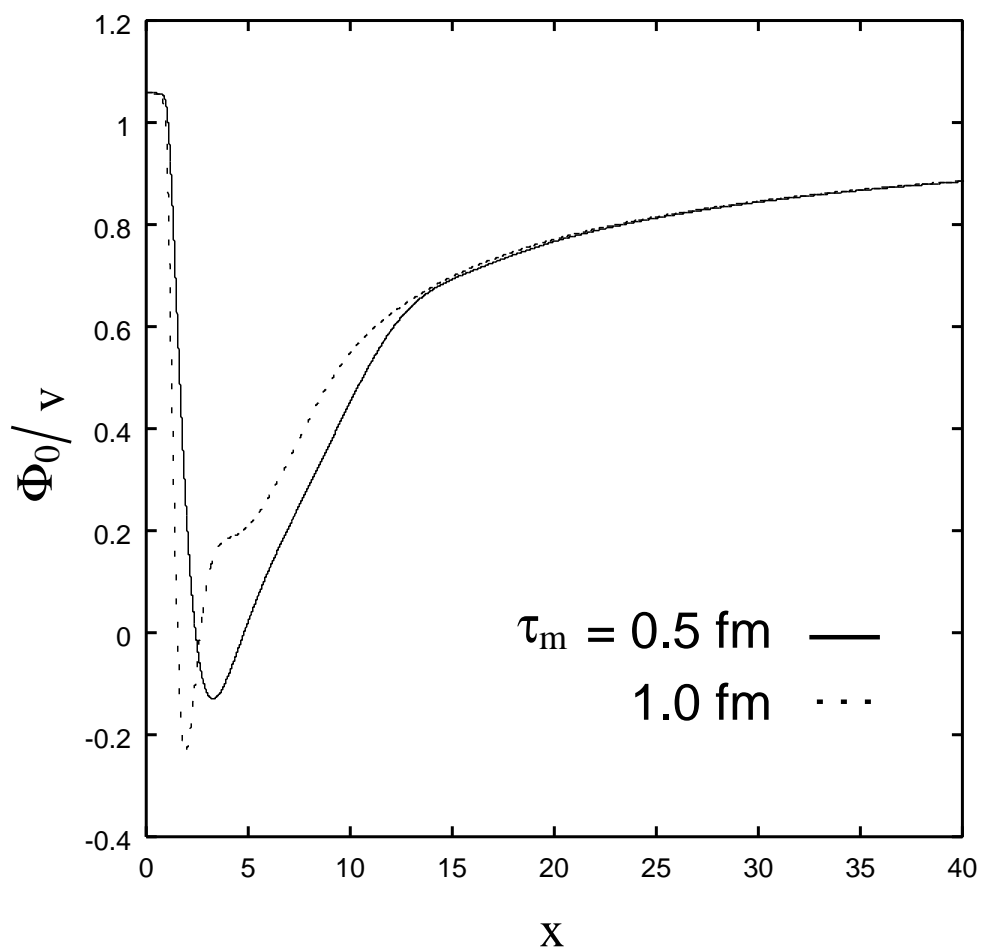


Fig.6



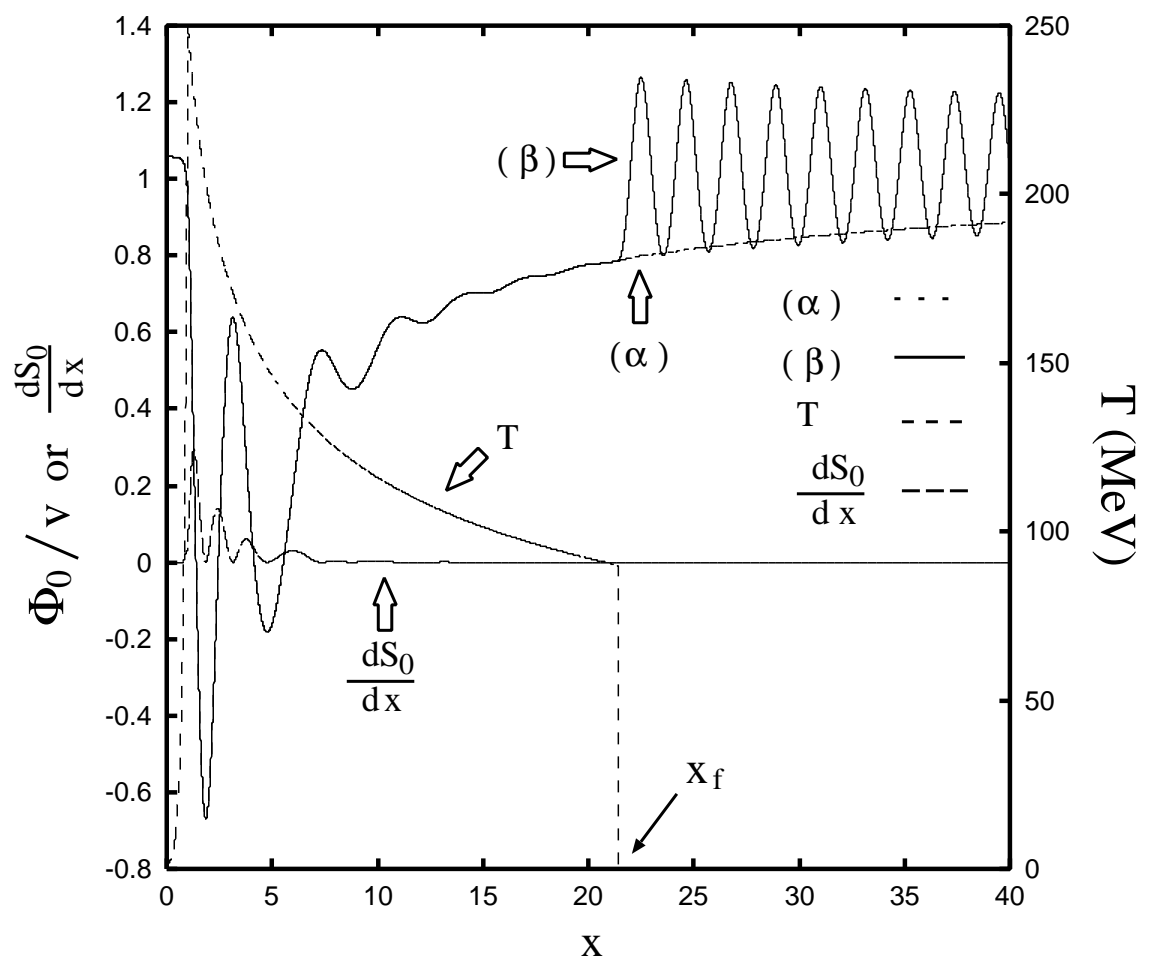


Fig.7



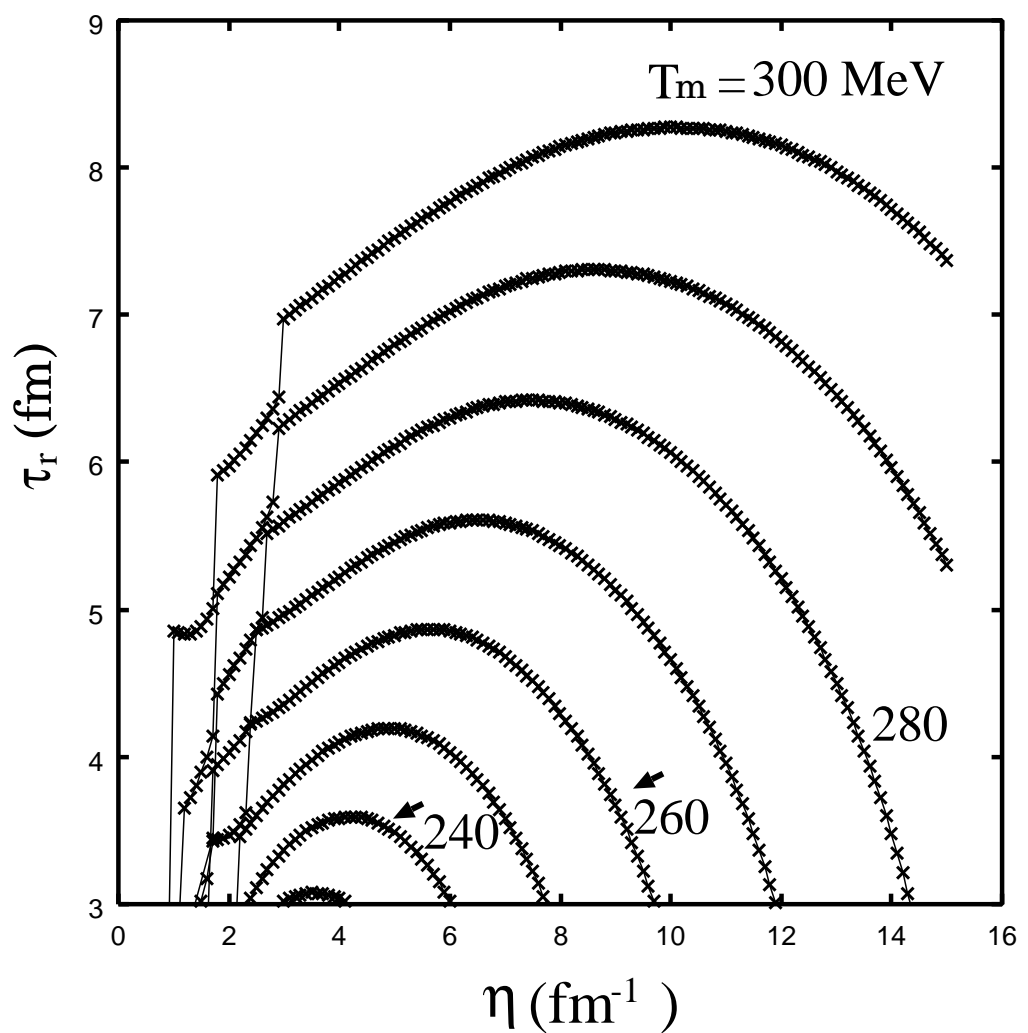


Fig.8



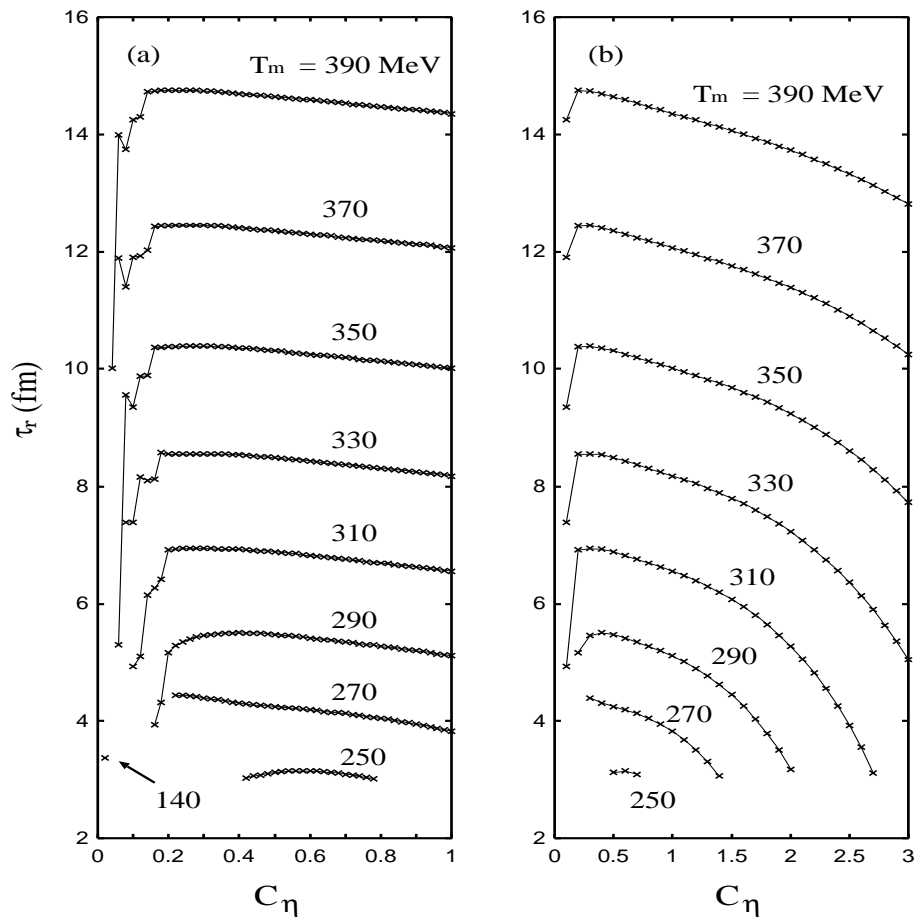


Fig.9



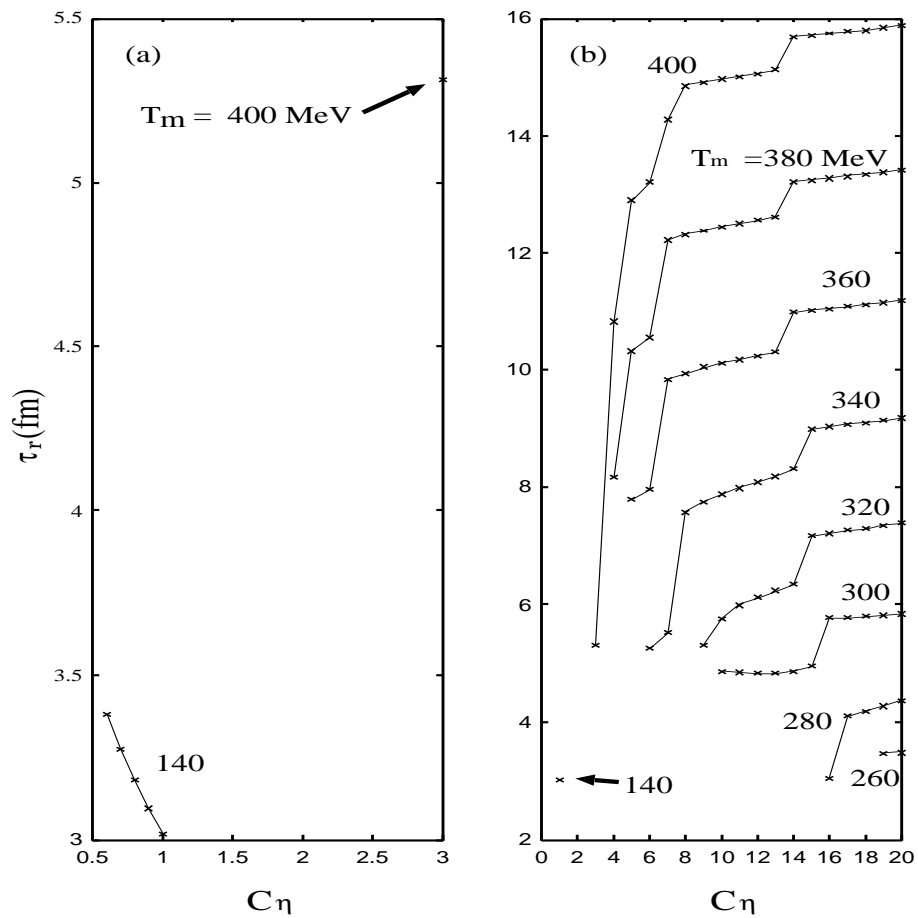


Fig.10



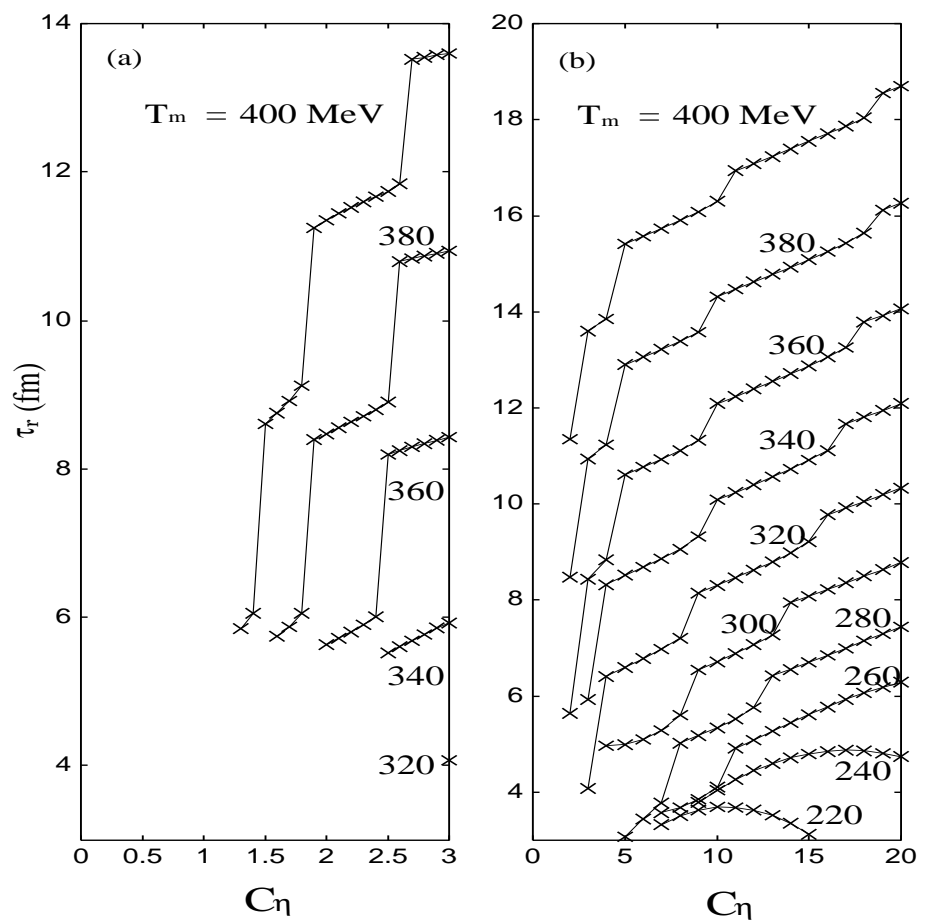


Fig.11



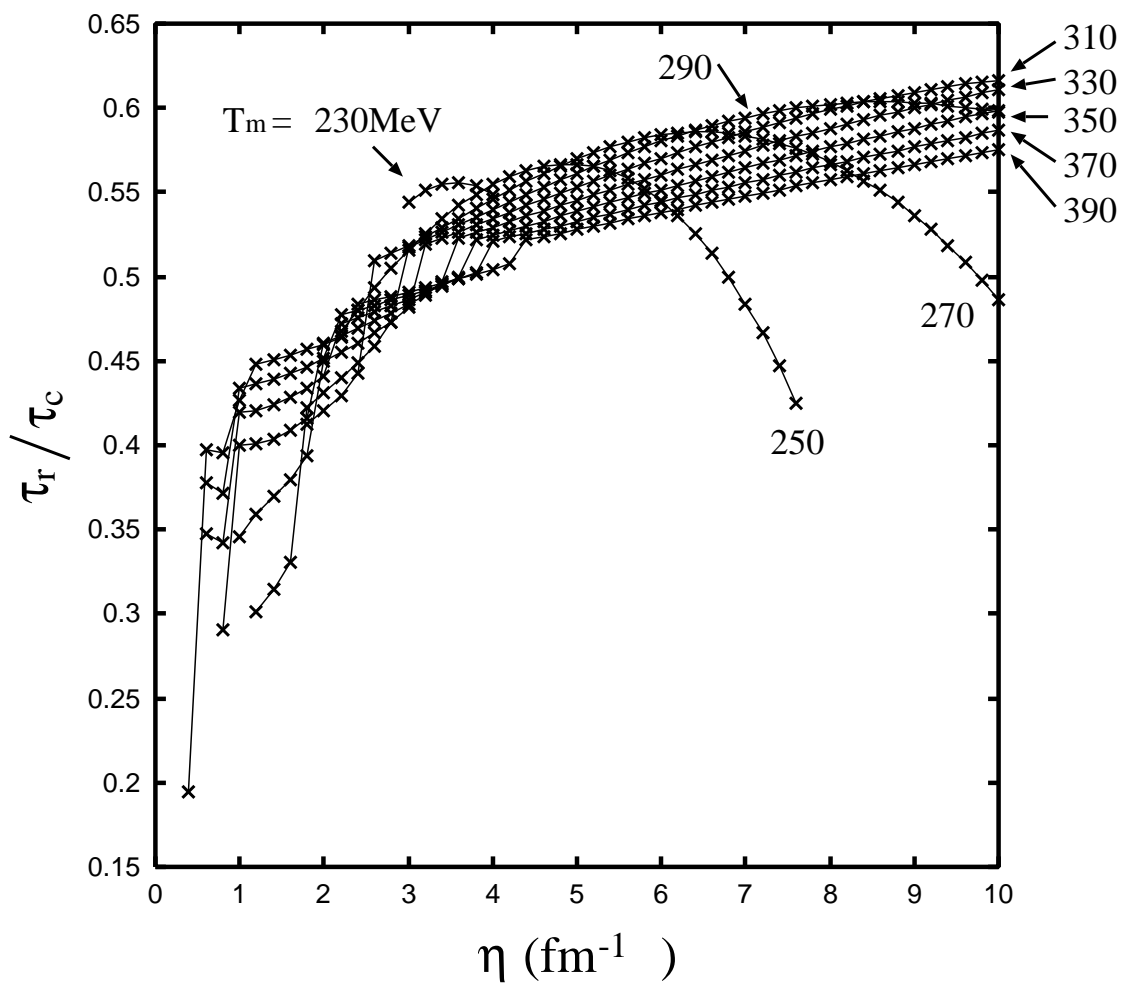


Fig.12



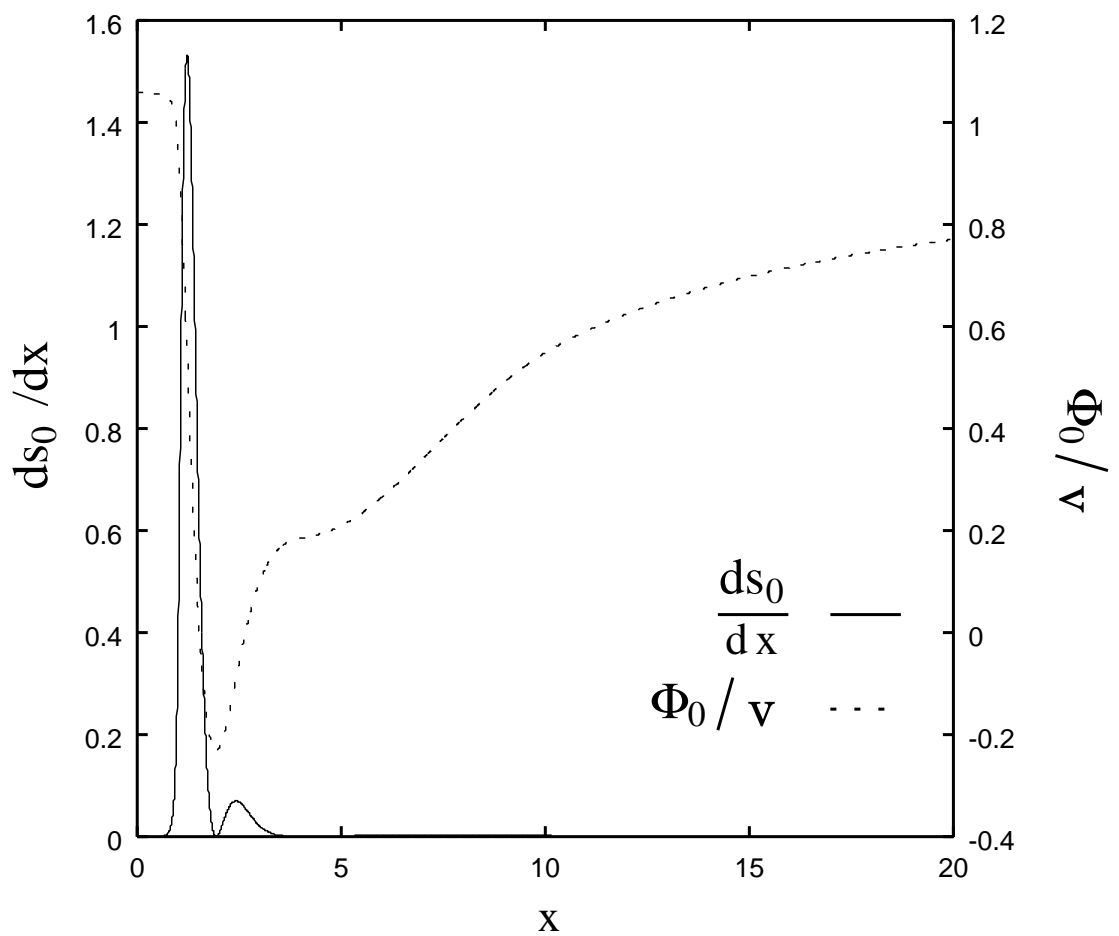


Fig.13

